

# Optimization of Three-Port Optomechanical Resonator Embedding a Meta-Surface Mirror

G. Ehrlich, R. Avrahamy, M. Auslender, S. Hava

Ben-Gurion University of the Negev, Department of Electrical Engineering, 653 Beer Sheva 84105 Israel

M. Zohar

Shamoon College of Engineering, Department of Electrical and Electronics Engineering, 950, Beer Sheva, 84100 Israel

**Abstract-** We studied a novel arrangement of two identical flat mirrors integrated with a nanograting mirror for coupling a  $-1^{\text{st}}$  diffracted order beam into a cavity circulation. The intracavity power buildup and combined throughput light power gain demonstrate high sensitivity to the cavity dimensions.

## I. INTRODUCTION

Among meta-devices [1], gratings are long known meta-surface devices capable of performing functions for nonconventional optics. Interferometry utilizes coherent addition of correlated optical waves, traditionally achieved by splitting and recombining a single optical beam entering through a transparent beam splitter. Yet, high-power light, used in some interferometric detectors, poses serious problems in transmission optics.

A concept for overcoming those problems with reflective optics alone was proposed, discussed [2] and implemented [3] for a standing-wave open Fabry-Perot (FP) cavity with two flat mirrors and a grating beam-splitter-mirror. Later, a ring travelling-wave FP cavity embedding similar elements was proposed [4]. Yet, no theory was elaborated in the open FP case [2,3], and only schematic treatment was presented in the FP ring case [4]. However, the grating was not optimized for best cavity gain. The present study aims at filling this gap, and this paper is devoted to the FP ring cavity.

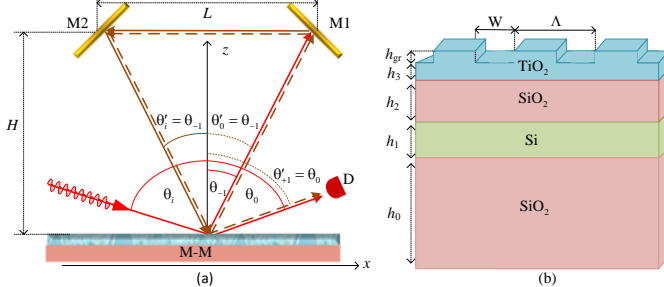


Fig. 1. (a) Travelling-wave grating based ring FP (GFP) cavity acting as described in the device operation mode tab; arrowed lines- light beams: Full – the incident, and first diffracted from meta-mirror (red) and reflected from the flat mirrors (brown); dashed – the circulating and added to the 0th order ray after each round trip. (b) The studied meta-mirror schematic.

## II. DESIGN OF A RING RESONATOR CAVITY

Consider an open FP cavity shown in Fig.1 (a), where M-M is the meta-mirror, which is a multilayer structure with a period  $\Lambda$  grating-patterned surface, as shown in the inset to Fig.1 (a); M1 and M2 are identical tilted flat mirrors arranged at a height H above M-M and located at a distance L from each other.

Let coherent light of a wavelength  $\lambda$  impinge M-M at an angle  $\theta_i$ . Then by properly setting  $2H/L$ ,  $\sin\theta_i - \lambda/\Lambda$  and the M1(2) tilts, one can force the initially diffracted  $-1^{\text{st}}$  order beam to launch the light circulation, so that after the first round trip the circulation proceeds indefinitely with the secondary 0<sup>th</sup> order beam. Simultaneously, the secondary out-of-cavity  $+1^{\text{st}}$  order beams, diffracted from M-M after each round trip, combined with the initial 0<sup>th</sup> order beam (as they propagate under the same angle), giving rise to the carrier light readout at the detector port D, as seen in Fig.1(a). The light recirculation results in an intracavity light power gain when the cavity is tuned and vice versa when it is detuned, as can be distinguished at the D readout.

## III. INTRACAVITY GAIN OPTIMIZATION

At  $H, L \gg \lambda$ , the travelling-wave nature of the ring resonator enables one to use geometrical optics, tracing the plane wave between the mirrors and at the cavity exit as straight zero-width rays. For the circulating resonant light power gain near M1, we obtain

$$G_{\text{res}} = \frac{|\rho_{-1}(\theta_i)|^2}{(1 - |\rho_0(\theta'_i)|R)^2}; \theta'_i = \theta_{-1} = \sin^{-1}\left(\sin\theta_i - \frac{\lambda}{\Lambda}\right) \quad (1)$$

where  $\rho_m(\vartheta)$  is the complex amplitude of  $m^{\text{th}}$  diffracted order, scattered by the grating when the impinging light is incident at an angle  $\vartheta$ , and R is the reflectance of the mirrors M1(2). The carrier light intensity at the detector port can be derived quite similarly. Finally, the ray-tracing analysis results are reasonably combined with the rigorous electromagnetic simulation of amplitudes  $\rho_m(\vartheta)$ , using our in-house software described in detail elsewhere [5].

We optimized the expression of  $G_{\text{res}}$  given by Eq.1, for a TiO<sub>2</sub>-air grating on a SiO<sub>2</sub> and Si multilayer stack shown in Fig.1(b). Using our multi-start optimization based simulation tools, we examined a wide range of the structure dimensions and incidence and diffractive reflection angles, to find the best structure for the above discussed use. The developed simulation tools are ready to be employed for optimization of any other grating-based cavity, be it open or closed, travelling- or standing-wave one, with components made of any known optical material.

## IV. RESULTS

For a TE polarized light with the wavelength  $\lambda_0 = 0.63\mu\text{m}$ , the optimization results peaked at  $\lambda_0$  with  $|\rho_0(\theta_{-1})| \approx 98\%$  in an extremely narrow Fano-like spectrum, as seen in Fig.2. This

serves well the light recirculation. The optimal grating-mirror structure dimensions and incidence angle are:  $h_1 = 1.9 \mu\text{m}$ ,  $h_2 = 2.7 \mu\text{m}$ ,  $h_3 = 0.7 \mu\text{m}$ ,  $h_{\text{gr}} = 0.3 \mu\text{m}$ ,  $\Lambda = 1 \mu\text{m}$ ,  $W = 0.3 \mu\text{m}$ , and  $\theta_i = 55^\circ$ , respectively.

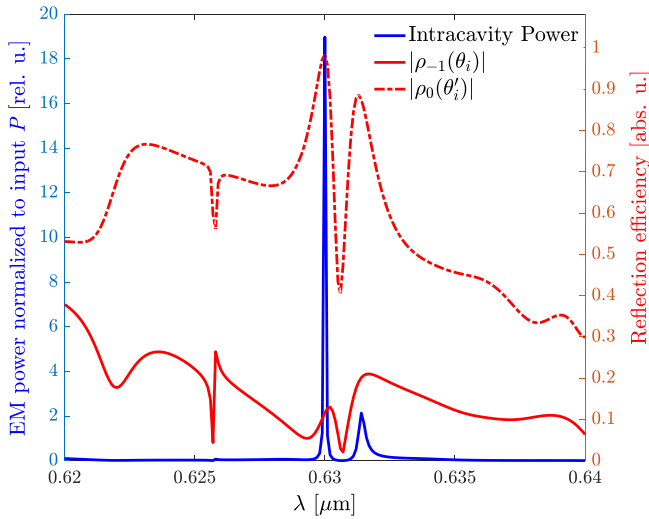


Fig. 2. The spectra of absolute values of initially diffracted  $-1^{\text{st}}$  and secondary  $0^{\text{th}}$  orders efficiencies (red), and the normalized intracavity power (blue) for the optimized structure described in the text above.

Fig.3 shows the carrier light yield and intracavity power gain, as functions of cavity dimension  $L$ .

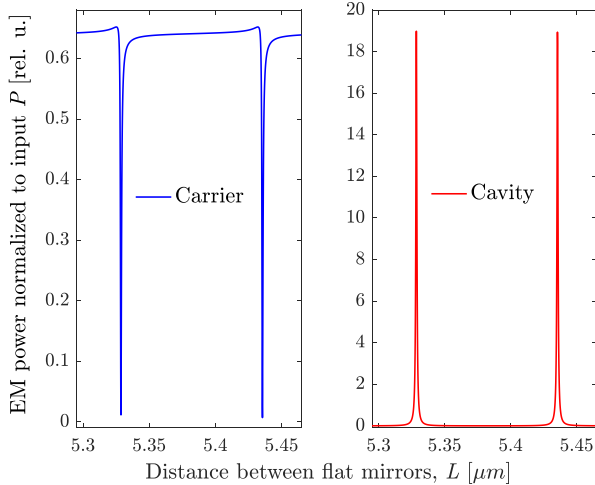


Fig 3. Carrier light yield and intracavity power as functions of cavity length  $L$  for the optimal structure under consideration.

### V. RAY ANALYSIS OF FINITE BEAM WIDTH

Any real light beam entering the cavity has a finite width. To extend ray tracing analysis to such beams, we approximated it as a continuous assembly of uncorrelated zero-width parallel rays, i.e. plane waves with the same optical-pass phase and independent random amplitude. Applying ray tracing to any ray of the above assembly, we obtained expressions of the intracavity and the out-of-cavity powers as functions of the displacement  $s$  of the ray from a central ray. Then, assuming the beam width to be  $\sigma$ , we integrated the power expressions

over  $s$  from  $-\sigma/2$  to  $\sigma/2$  to obtain the contribution of the entire beam. The averaged intracavity power vs.  $L$  for several values of  $\sigma$  is shown in Fig.4.

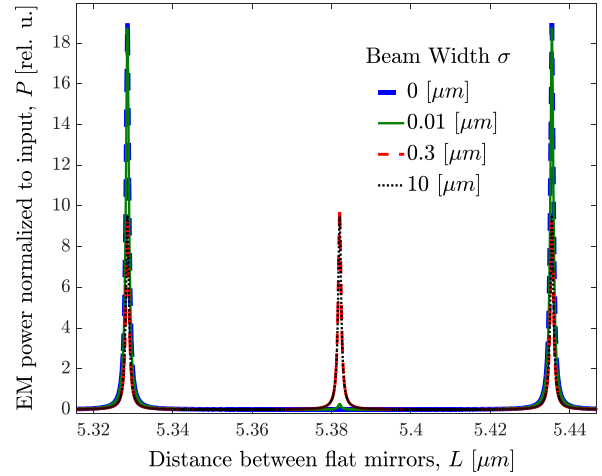


Fig 4. Intracavity light power yield as a function of cavity length for increasing beam width.

### VI. DISCUSSION AND CONCLUSION

As can be seen from Fig.2 and Fig.3, the designed grating embedded FP ring cavity has high finesse and throughput contrast for both wavelength and cavity dimensions. It appears that deviation of the incidence angle from the designed  $\theta_i$ , detunes the cavity from resonance, and therefore leads to a very high sensitivity in  $\theta_i$  as well. Furthermore, the high finesse, as seen in Fig.4, and the sharp throughput contrast (not shown), both with respect to  $L$  are kept for rather wide beams, which is important in terms of realistic detection instruments. Comparing Fig. 3 and 4, one can see that finite beam width causes additional cavity resonances between the resonances of the zero-width ray. This is due to the return of all off-center ray to their initial incidence spot only after two round trips.

To conclude, we studied a novel arrangement of two flat mirrors and nanograting mirror for coupling  $-1^{\text{st}}$  diffracted order beam into an open travelling-wave cavity circulation. The intracavity power buildup and combined throughput light power gain demonstrate high sensitivity to cavity dimensions. Thus, the considered optomechanical meta-device resonator can serve as a highly sensitive position detector, mode cleaner or mode combiner.

### REFERENCES

- [1] N.I. Zheludev and Yu.S. Kivshar, "From metamaterials to metadevices," Nature Mater. 11, 917, 2012.
- [2] K.-X. Sun and R. L. Byer, "All-reflective Michelson, Sagnac, and Fabry-Perot interferometers based on grating beam splitters," Opt. Lett., 23, 567, 1998.
- [3] A. Bunkowski, O. Burmeister, K. Danzmann, R. Schnabel, T. Clausnitzer, E.-B. Kley, and A. Tünnermann "Demonstration of three-port grating phase relations," Opt. Lett. 31, 2384, 2006.
- [4] R. Schnabel, A. Bunkowski, O. Burmeister and K. Danzmann, "Three-port beam splitters-combiners for interferometer applications," Opt. Lett. 31, 658, 2006.
- [5] M. Auslender, A. Bergel, N. Pinhas and S. Hava, "Multi-layered grating diffraction, graphical user interfaced simulation toolbox in the MATLAB environment," Proc. SPIE 5349, 463-473, 2004.